Photo or figure (optional)

Calculation of displacements of measured accelerations, analysis of two accelerometers and application in road engineering

Martin Arraigada, Empa, Road Engineering/Sealing Comp.
Manfred Partl, Empa, Road Engineering/Sealing Comp.

Conference paper STRC 2006

STRC

6th Swiss Transport Research Conference
Monte Verità / Ascona, March 15. – 17. 2006

Calculation of displacements of measured accelerations, analysis of two accelerometers and application in road engineering

Martin Arraigada
Road Eng. / Sealing Components Laboratory
Empa - Material Science & Technology
CH-8600 - Dübendorf

Phone: 044 8234213
Fax: 044 8216244
email: martin.arraigada@empa.ch

Manfred Partl
Road Eng. / Sealing Components Laboratory
Empa - Material Science & Technology
CH-8600 Dübendorf

Phone: 044 8234113
Fax: 044 8216244
email: manfred.partl@empa.ch

March 2006

Abstract

In-situ vertical deformation of the different pavement layers due to traffic loads is essential information for assessing the effect of freight vehicles on the structural behaviour of a road. In order to determine the deflection of a road, LVDT are usually installed. However, this method is quite complicated and tedious. As an alternative, and as part of an ongoing research project, the feasibility of using accelerometers to measure road deflections is investigated in this paper. The paper discusses problems involving the calculation of deflections from acceleration recordings (double integration) due to the amplification of measurement errors of the acceleration signal. Results of two experiments, one laboratory test and one full scale wheel tracking test are presented. Two accelerometers from different manufacturers were tested in the lab using “road like” vibrations and one was used in the wheel tracking test. Deflections were calculated from measured accelerations using an algorithm to correct errors due to double integration.

Keywords

pavement in-situ measurements - pavement deflection - accelerometers

1. Introduction

The use of deformation sensors to measure the deflection of pavement layers due to traffic loads is difficult and often involves complex installation procedures. Since absolute deflections can only be obtained with reference to a fixed point it is necessary to anchor the sensor in great depth under the road structure. Unlike deflection, acceleration is always an absolute value that refers to the state of "no acceleration" as fixed point. Hence, anchor in great depth is not necessary in this case. The reduced size and robust construction of many existing sensors adds to the simplicity of measurements. Last but not least, costs of measuring with accelerometers are low and decreasing. For all these reasons using accelerometers for evaluating deflections within a road structure appears promising and attractive.

However, the main difficulty in applying this procedure is that acceleration traces must be numerically integrated in order to obtain first velocity, and after a second integration, displacement (and therefore road deflections). Numerical double integration of measured accelerations involves errors that must be carefully studied and minimized: time integration amplifies the low frequency components of the signal and any measurement error is significantly amplified (Feltrin et al, 2004). Unfortunately, digital recordings of accelerations usually comprise so called baseline offsets: small steps or distortions in the reference level of motion (Boore et al, 2002). Consequently, velocity and displacement traces obtained by integrating the recorded accelerations are commonly flawed by drifts that produce unrealistic results (Boore, 2005) (Iwan et al, 1985). The origin of these acceleration offsets is diverse and can be classified in errors due to instrumental instability (non linear instrument response, limited resolution of the measuring system, insufficient sampling rate, level of electronic noise), background noise (depending on the measuring site), the estimation of the real initial acceleration, velocity and displacement values and data manipulation (Chiu, 1997) (Boore, 2003).

Experiments summarized in this paper focus on investigating the feasibility of using accelerometers instead of deformation sensors in the road. However, before conducting the experiments it was necessary to define the required features of the sensors. As to answer the question: which sensor and measuring system are most suitable for minimizing such long period noise after integration?

The characteristics of the vibration produced by a heavy vehicle within a pavement structure depend on many factors. In general, signals with low frequency contents and small amplitudes might be expected and detection of small vibration signals with good accuracy requires a sensor with low self-noise. Following these principles, the authors of this paper selected two commercially available high-resolution accelerometers. Desirable features such as compact

size, low noise, low frequency response and high shock tolerance are often contradictory requirements for the design of an accelerometer, but are the main features of the selected devices. In order to evaluate their performance in the laboratory, the sensors were tested using a horizontal vibration exciter.

After selecting one of the sensors, another experiment was carried out at the ETH - IGT Circular Pavement Test Truck (CPTT) in Dübendorf. The sensors were installed in the surface zone of five pavement structures and measurements were performed for different tire speeds. Deflection of the structure under the tire loads was then calculated using time numerical integration.

2. Theoretical and measuring technique aspects

2.1 Acceleration, velocity and position

Vibration is a mechanical oscillation or motion of an object around a reference point of equilibrium. It can be measured in terms of displacement, acceleration and velocity over time. These parameters are closely related to each other: if the measured parameter is acceleration, the other two can be found through a single and double integration. On the other hand, acceleration and velocity can be calculated from displacements through single and double differentiation. The conversion process can be implemented in either hardware by using analog integrators or software by performing digital integration. Mathematically, the calculation of displacements $d_c(t)$ from a measured acceleration $a(t)$ is simple:

$$d_c(t) = d_0 + v_0 t + \int_0^t dt \int_0^\tau a(\tau) d\tau \tag{1}$$

where:

d_0 : initial displacement, $t = 0$

v_0 : initial velocity, $t = 0$

d_c : calculated displacement, t

This formula is used for continuous (analog) functions. Today almost all signals are discrete (digital) and integration must be numerical. Displacements from numerical integration of the digital acceleration and velocity signals (waveforms) can be computed with different methods. Basically, all the available numerical techniques for integration calculate the area under the graph of the discrete function over time. Figure 1 illustrates the simple trapezoidal method, where the region under the analog signal is approximated by the sum of a series of rectangles. The time increment between samples Δt depends of the measurement sampling frequency, in other words depends on how often the analog signal $a(t)$ is digitalized. The Δt step must be small enough to approximate signals with “high curvature” minimizing the calculation error. This means that the sampling frequency should be high enough in relation to the highest frequency content of the waveform.

Figure 1 Numerical integration using the trapezoidal method.

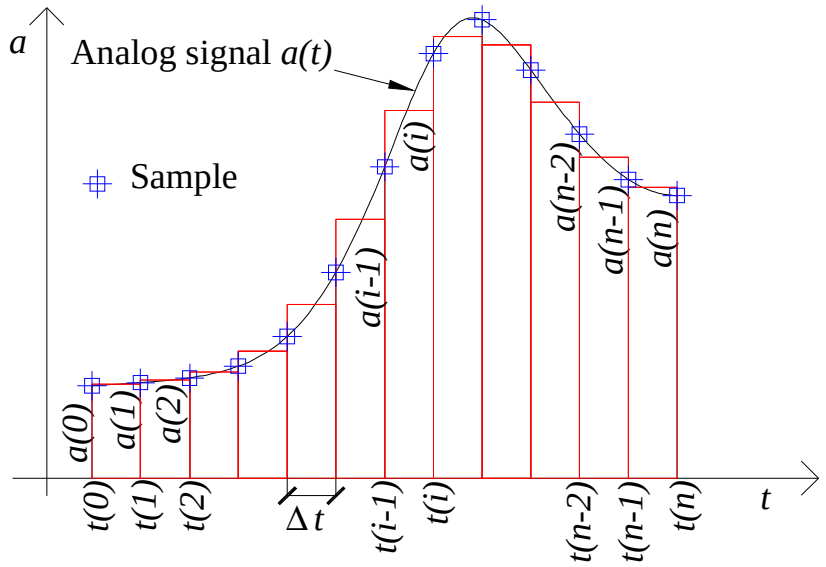

The integration of a discrete signal in the time domain is then calculated numerically as follows:

$$\int_{t(0)}^{t(n)} a(t)dt \cong \sum_{i=1}^{n}\left(\frac{a(i-1)+a(i)}{2}\right)\Delta t \tag{2}$$

where:

a (t) : continuous time domain waveform

a(i) : i^{th} sample of the time waveform

Δt : time increment between samples (*t(i)-t(i-1)*)

n : number of samples of the digital record

Thus, displacements can be calculated recursively in two steps, first computing velocity from acceleration and then, displacement from velocity:

$$v_c(i) = v_c(i-1) + \frac{a(i-1)+a(i)}{2}\Delta t \tag{3}$$

$$d_c(i) = d_c(i-1) + \frac{v(i-1)+v(i)}{2}\Delta t \tag{4}$$

where:

$a\ (i)$: i^{th} sample of the acceleration waveform

$v_c\ (i)$: i^{th} sample of the calculated velocity

$d_c\ (i)$: i^{th} sample of the calculated displacement

2.2. The problem of time integration

Although time integration seems to be straightforward, there are hidden difficulties that can spoil the final results. When integrating, low frequencies contents of the waveform are strongly amplified, high frequencies are reduced and the phase is changed. Thus, the greatest problem in calculating displacements from accelerations is that any offset of the acceleration signal (constant or very slowly changing value) will dominate the results of the calculated displacements.

The following simple numerical example shows the effect of double integration of a periodic waveform (units of acceleration were added in order to get a better feeling about the magnitudes involved). The first function to be integrated, $a_1(t)$, is the result of the sum of two periodic functions: two sine with frequencies of 0,5Hz and 10Hz and an amplitude of 0,1m/s2. The second function $a_2(t)$ is composed by the same two sine as $a_1(t)$. However, in this case a small constant offset of - 0,01m/s2 was added. In order to integrate the functions numerically, samples were calculated every 0,01s (it means that the "sampling frequency" was set to 100Hz, i.e. 10 times higher than the highest frequency content of the function). Both digital waveforms a_1 and a_2 are shown in the upper graph of Figure 2. The offset is displayed as an amplitude shift in both signals.

The middle graph on the same figure presents the calculated velocities v_{c1} and v_{c2} from the numerical integrated accelerations a_1 and a_2 respectively. For the calculations it is assumed that the initial velocity is zero. It can be seen that v_{c1} presents a constant offset (in the figure, Baseline v_{c1}). As a result of the constant offset added to a_2, the integration resulting in v_{c2} presents a linear drift (Baseline v_{c2}). For both calculated velocities the high frequency content of the original acceleration waveforms has strongly diminished.

The lower graph of Figure 2 contains the calculated displacements dc1 and dc2 after the integration of the velocities v_{c1} and v_{c2} respectively. Initial displacements were set to zero. The results show that the higher frequency acceleration produces unnoticeable displacements compared to the low frequency acceleration. Due to the integration of the velocity offset (Baseline v_{c1}), the baseline of d_{c1} presents a linear drift and the calculated displacement after

4s is 133mm. On the other hand d_{c2} presents a quadratic baseline (Baseline d_{c2}) caused by the integration of the linear drift of baseline v_{c2}. The final displacement, considering 4s is 213mm. Between both calculated displacements there is a difference of 80mm after 4s. This simple example clearly demonstrates that even a little constant offset error in the measured acceleration may produce a significant linear trend on the calculated velocity and a quadratic baseline error on calculated displacements. In addition, the correct evaluation of the initial conditions regarding acceleration, velocity and displacement are essential to obtain realistic results. A detailed theoretical study about the effects of time integration can be found in (Feltrin et al, 2004).

2.3. Aspects of sensors and measurement technique

As previously discussed, low frequency contents dominate the results of the double integration. Thus, it is important to prevent measuring errors at these frequencies as they would be amplified in a way that could completely alter the results. The characteristics of the measuring system should be selected properly in order to minimize any possibility of propagation and amplification of these errors.

In that case, what kind of sensors should be used? Which desirable features should they have? In order to answer these questions it is important to know the nature of the loads and how they affect the pavement structure.

There are many factors influencing the dynamic deformation of the road, but normally it is likely to find very small deformations at low frequencies. Small deformation amplitudes at low frequency produce very little acceleration. For example, a harmonic vibration of frequency ω and displacement amplitude d_{max}, results in a maximum acceleration a_{max} calculated as follows:

$$a_{\max} = d_{\max}\omega^2 \tag{5}$$

Let's assume a situation on the road where a truck passes at 70km/h and the maximum displacement (deflection) d_{max} produced by one of its tires is 0.02mm. Considering that the size of a "sine like" deformation basin has a diameter of 6m, the truck is displacing a point in the pavement downwards during 0.309s; this corresponds to a 1.6Hz wave (ω=10,18 rad/s). The maximum acceleration a_{max} calculated with equation (5) is then 211µg. In order to measure this kind of vibration a resolution of ca. 70µg is necessary. Hence, for this hypothetical situation a high sensitivity, high-resolution sensor capable to measure low frequency vibrations is required.

Figure 2 The top graph shows the time histories of two periodic acceleration waveforms a_1 and a_2. Both contain the sum of two sine functions of the same amplitude and different frequencies (0,5Hz and 10Hz), but a_2 additionally includes a very small offset of -0.01m/s2. The middle diagram contains two traces corresponding to the numerically calculated velocities. The difference in the baselines v_{c1} and v_{c2} reveals the influence of the added offset as now baseline v_{c2} presents a linear drift. The contribution of the 10Hz acceleration sine produces small velocity amplitudes. Resulting displacements in the lower graph exhibit a difference of 80mm after 4s, the baseline d_{c2} is now quadratic.

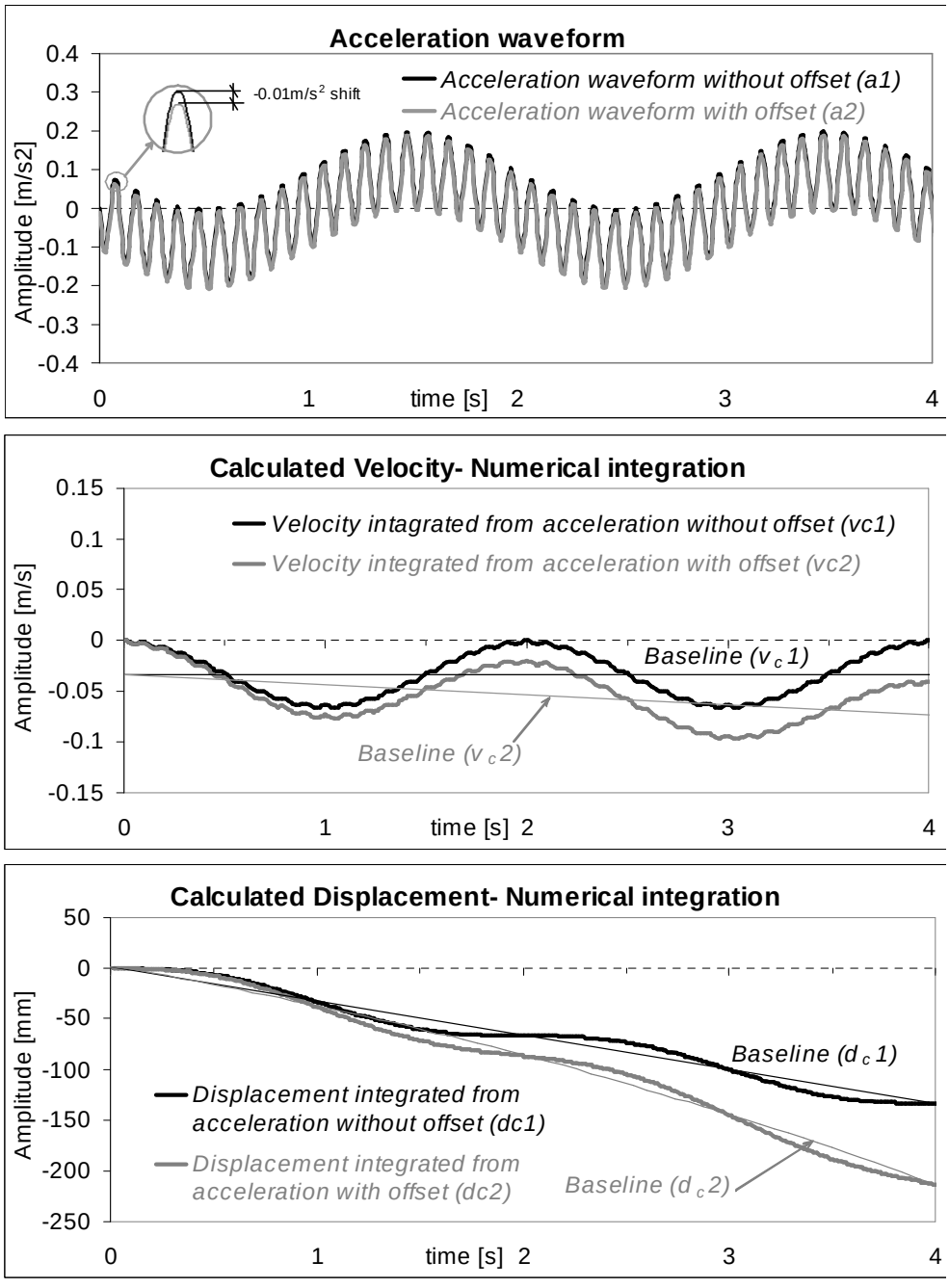

Recently, so-called capacitive accelerometers appeared in the market manufactured by surface micromachining technique. This technique allows lower costs and smaller sizes (Shieh et al, 2001). The all-in-one package design minimizes the problems of noise and non-linearity. Typically these devices have a good bandwidth with low frequency response (down to 0Hz), a wide dynamic range and high resolution. They may be suitable for road applications where the expected deflection amplitudes are rather small and the frequency contents low.

However, due to the tiny seismic mass of these sensors and the inevitable internal noise, the following questions arise: how precise are the sensors for measuring small deflections at low frequencies? Can these sensors accurately measure the small accelerations produced by the traffic? Do these sensors have baseline offsets capable to spoil a double integration calculation? To answer these questions, two commercially available accelerometers with similar characteristics were tested in the laboratory.

3. Sensor features

The most important features of the two chosen accelerometers PCB series 3700 and Applied MEMS model SF1500L[1] (hereafter referred as PCB and MEMS respectively) are summarized in Table 1 in terms of sensitivity, measuring and frequency range and resolution[2].

Table 1 Characteristics of evaluated sensors according to manufacture's specifications

ACCELEROMETER	PCB	MEMS
Sensitivity (±5 %)	1000 mV/g	1200 mV/g
Measurement Range	±3 g pk	±3 g pk
Frequency Range (±10 %)	0 to 150 Hz	0 to 5000Hz
Noise (10Hz) [Resolution]	4 µg /√Hz [41µg]	300 ng/√Hz [3µg]

In addition to the high sensitivity, low frequency response and high resolution of both sensors, their small size and weight are also remarkable characteristics with respect to the intended application in asphalt pavements.

[1] Recently the company Colibrys acquired part of Applied MEMS. Former Applied MEMS sensors are now Si-FlexTM.

[2] Different manufactures use different parameters to define their sensor's properties in the product's datasheets. The resolution of the sensor is defined as the smallest change in stimulus that will produce a detectable change in instrument output. Hence the amplitude of the expected signal should be higher than the resolution of the sensor. Resolution is related to the concept of noise floor (sensor inherent electrical noise that is superimposed on the actual signal). As a rule of thumb, the smallest detectable signal must be 10dB higher than the noise floor. Although PCB provides the information in terms of Broadband rms resolution (30 µg), Table 1 includes the formula of the narrowband spectral noise at 10Hz. In brackets the calculated resolution considering the specification formulas and the 10dB rule is given

4. Laboratory tests

4.1 Setup

The objective of these tests was to evaluate in the laboratory the probable performance of the accelerometers regarding road deflection measurements under heavy vehicle passing.

For that purpose, PCB and MEMS accelerometers were attached to a moving plate that operated as a shaking table, and a horizontal servo hydraulic cylinder was used to excite the plate (see Figure 3). Available deflection data collected from road measurements *d(t)* were used to simulate a passing truck. These data were available thanks to the measurements of the magnetostrictives deformation sensors installed on a Swiss motorway (Raab et al, 2002) (Raab et al, 2003). The selected data correspond to a test truck used to "calibrate" the deformation sensors.

The vibration of the moving plate attached to the servohydraulic cylinder was measured with both transducers. The real displacement of the plate was simultaneously monitored with an inductive displacement sensor (LVDT) fixed to the ground.

Figure 3 Schematic testing setup.

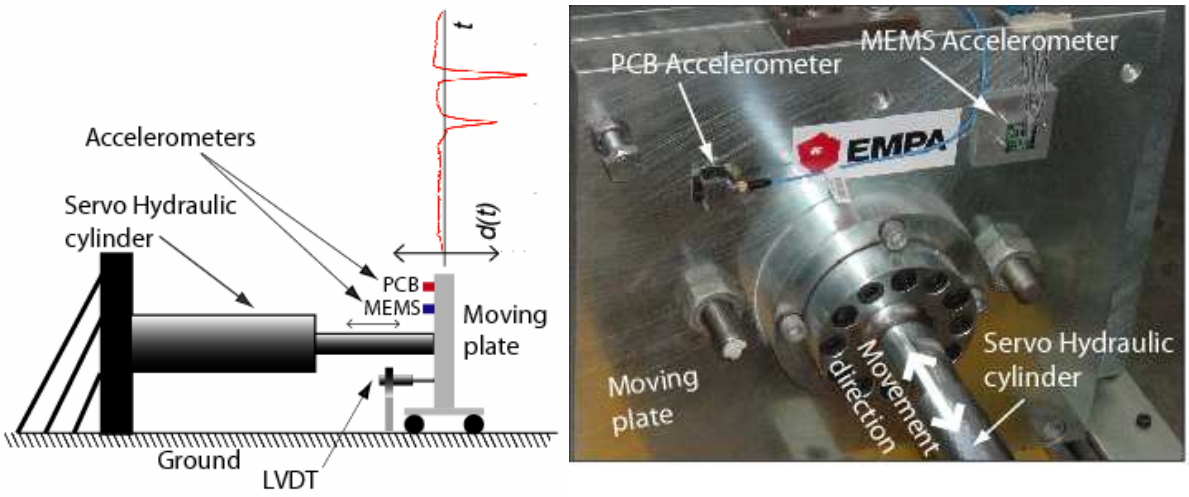

4.2 Command Signal

The deflection signal corresponds to a 17ton truck (first axle 4.5ton, second axel 12.5ton) passing by the sensor at a speed of 20km/h. The signal indicates the relative displacement

between the magnet M2 at -12cm and the sensor anchor at -4cm, representing the total deformation of the second pavement's layer. These data were obtained from measurements with a well defined "calibration truck" on an instrumented Long Term Pavement Performance (LTPP) section on the heavily trafficked Swiss motorway A1 between Zurich and Bern (Raab et al, 2002) (Raab et al, 2003).

The measured deflection data ("raw data") draw (t) is depicted on the upper graphic of Figure 4, showing the pavement vertical deformation produced by the two axles of the truck during the passing event. In order to "clean" the signal of high frequency noise, a low pass filter with a cut off frequency of 20 Hz was applied (see middle graphic in Figure 4). The resulting filtered deflection $d_{filt}(t)$ has a maximum for each axle of about 0.06mm and 0.09mm respectively, and the time vector has a length of 3.6s. As these values are too small to be reproduced using the servohydraulic cylinder, the trace was scaled in time and amplitude, taking care in having the same acceleration levels for both signals, scaled and not scaled. This was done using a scaling factor of 202 for amplitude and 20 for time applied (see lower graphic in Figure 4). As a result, the filtered and scaled signal $d_{filt\text{-}sc}$ shows a maximum displacement of 36mm and the resized time vector a length of 71s. As d_0 and d_f (initial and final displacement) were not zero, it was necessary to add two 5s ramps at the beginning and end of the trace, taking care of the fact that the acceleration resulting from the derivation of these ramps was smaller than at the rest of the signal. The result is the signal used to feed the moving plate, called command signal. The "real" or "true" displacements of the plate relative to the ground were measured with the inductive displacement sensor (LVDT).

Figure 4 Conditioning of the raw deflection signal to obtain the command signal after filtering and scaling.

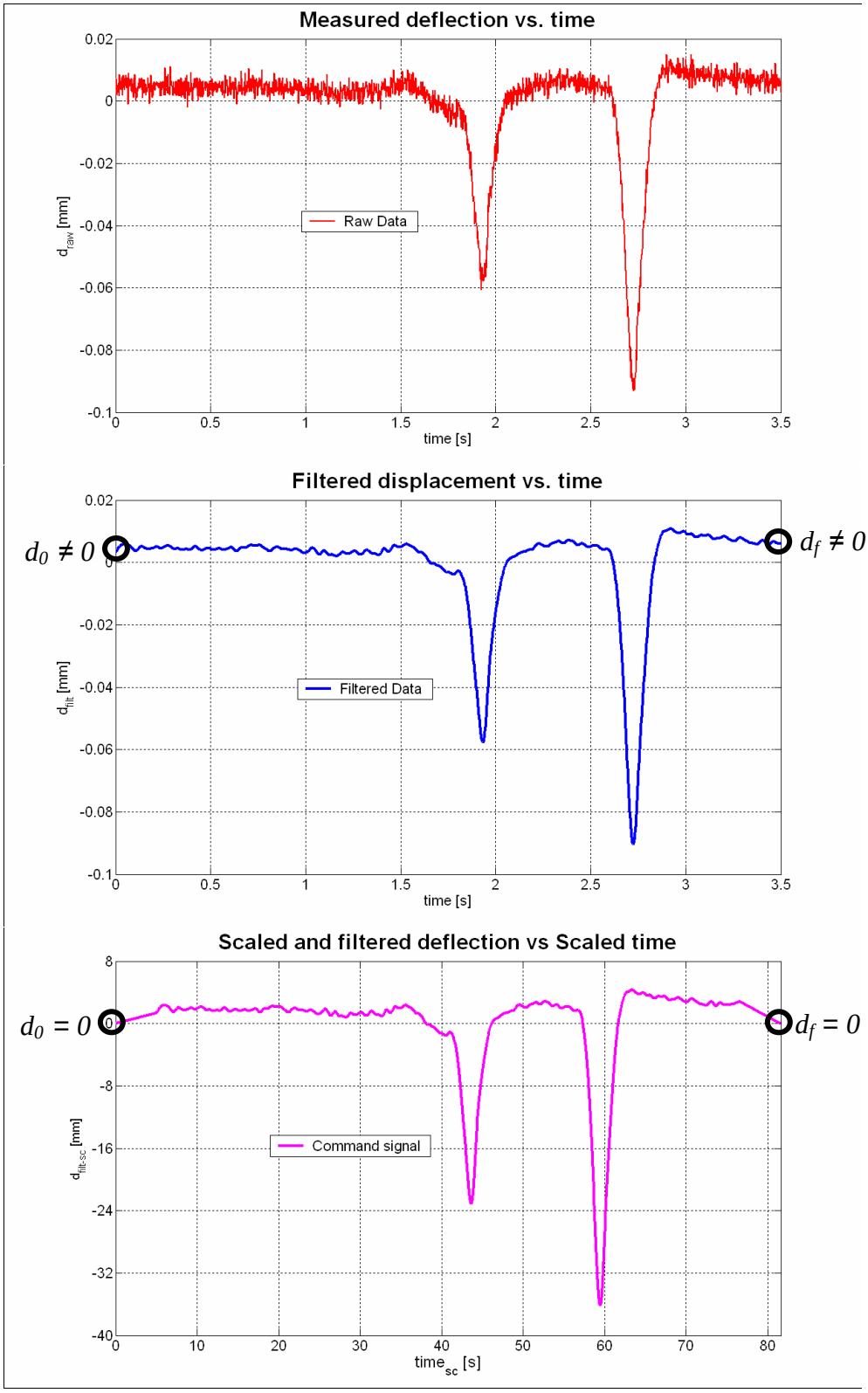

4.3 Experimental program

Measurements were repeated four times, as indicated in Table 2. In order to evaluate the influence on the numerical integration, two different sampling rates were analyzed. The acceleration measurements were triggered manually, before starting the tests. The duration of the measurement was selected to 100s, enough to acquire the whole event of 83s.

Table 2 Measurement program.

Meas N°	Sampling rate [Hz]	Duration [s]	Range [mV]	Ch1	Ch2
1	1024	100	175	PCB	MEMS
2	1024	100	175	PCB	MEMS
3	2048	100	175	PCB	MEMS
4	2048	100	175	PCB	MEMS

4.4 Results

The acceleration traces for both accelerometers for measurement N°4 are shown in the upper part of Figure 5. The lower part of Figure 5 presents the corresponding Power Spectrum (PS) of the signals. The only correction applied to the recorded motions was the removal of the mean of a portion of the pre-event trace, subtracting it from the whole record. No high pass or low pass filtering was applied to the signal since no improvement was obtained in this case due to the fact that it is not possible to construct a stable filter with an exact cutoff frequency. Consequently, filtering causes a loss of important information, producing an alteration of the recorded data and the corresponding calculated displacement. The PS analysis, on the bottom of Figure 5, shows the strength of the different frequencies that form the signal. In other words, it describes how the power carried by the signal is distributed in frequency. The highest spectral components of both, PCB and MEMS signals, are between 5Hz and 60Hz, and have maximum peaks at 31Hz and 35Hz. Another peak is around 100Hz, probably due to noise induced by the hydraulic mechanism governing the movement of the plate.

Figure 5 Acceleration time signals and Power Spectrum (PS) of meas N° 4.

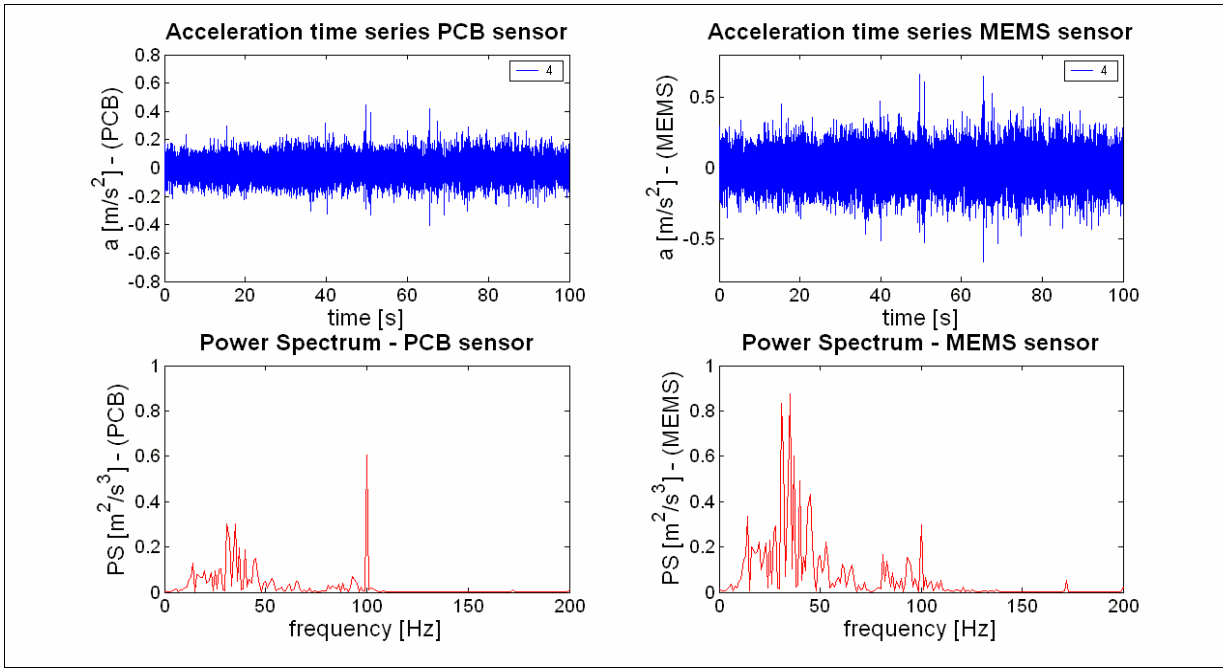

Following the recursive procedure described in equations (3) and (4), displacements were reconstructed from acceleration time series. Figure 6 shows the results for PCB and MEMS accelerometers, for test 2 and 4. Although Figure 6 confirms that there is a good agreement between the command signal and the calculated deformation in the region of the passing tires, the results are flawed with random drifts as a consequence of the amplification of acceleration baseline offsets after double integration. The baseline drifts seems to have higher amplitudes in the case of integrating MEMS acceleration data.

How can these drifts be removed in order to get the real displacements? Many baseline correction techniques for seismic acceleration recordings are proposed in the literature (Iwan et al, 1985) (Chiu 1997) (Boore 2001) (Boore et al, 2002). In the present analysis, the displacement traces were corrected using a high-order polynomial $p_n(t)$ to approximate the displacement drift (Feltrin 2004). The polynomial is fitted to the rectified calculated displacements $d_{c\text{-}rec}(t)$. During the events (tire passes of the two axle truck) the calculated displacement $d_c(t)$ is replaced using a linear interpolation (see Figure 7 and Figure 8). In this investigation, initial and final points for each event defined as t_1, t_2, t_3, t_4 were assigned manually. As a result $d_{c\text{-}rec}(t)$ tends to follow the displacement drift, which is approximated by the polynomial function $p_n(t)$ (see Figure 9). Then, the originally calculated displacement vector $d_c(t)$ is subtracted to the polynomial function obtaining the corrected displacement vector $d_{cc}(t)$ (see Figure 10). Hence, the following expression is used:

$$d_{cc}(t) = d_c(t) - p_n(t) \tag{6}$$

No high pass filtering was applied, as its implementation damaged the records and produced unrealistic results

Figure 6 Displacements obtained by double integration, for both sensors during test 2 and 4. Integrated traces show drifts due to the effect of the acceleration baseline offsets.

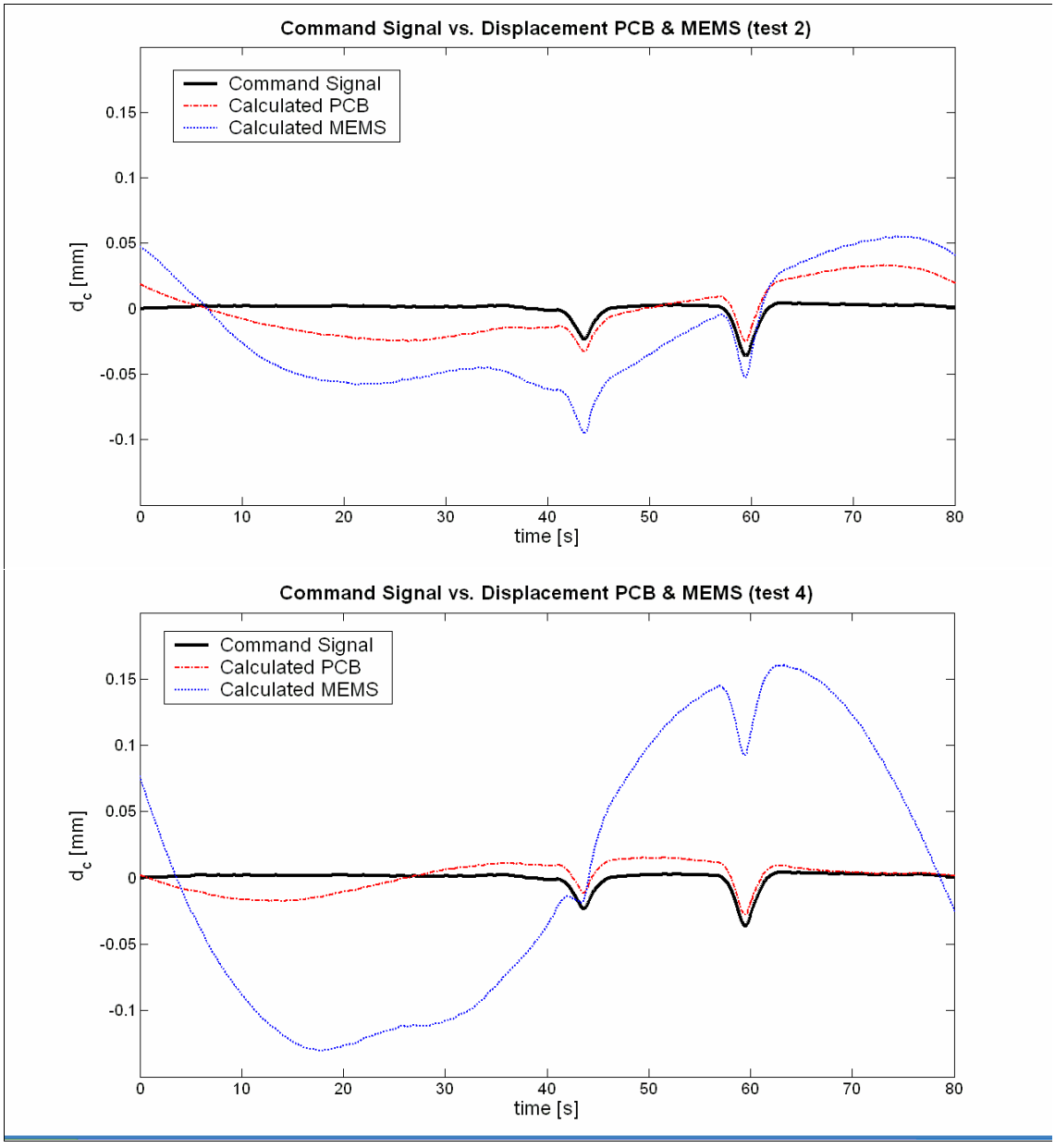

Figure 7 Results for test N4, PCB sensor. Calculated displacement $d_c(t)$ vs. command signal.

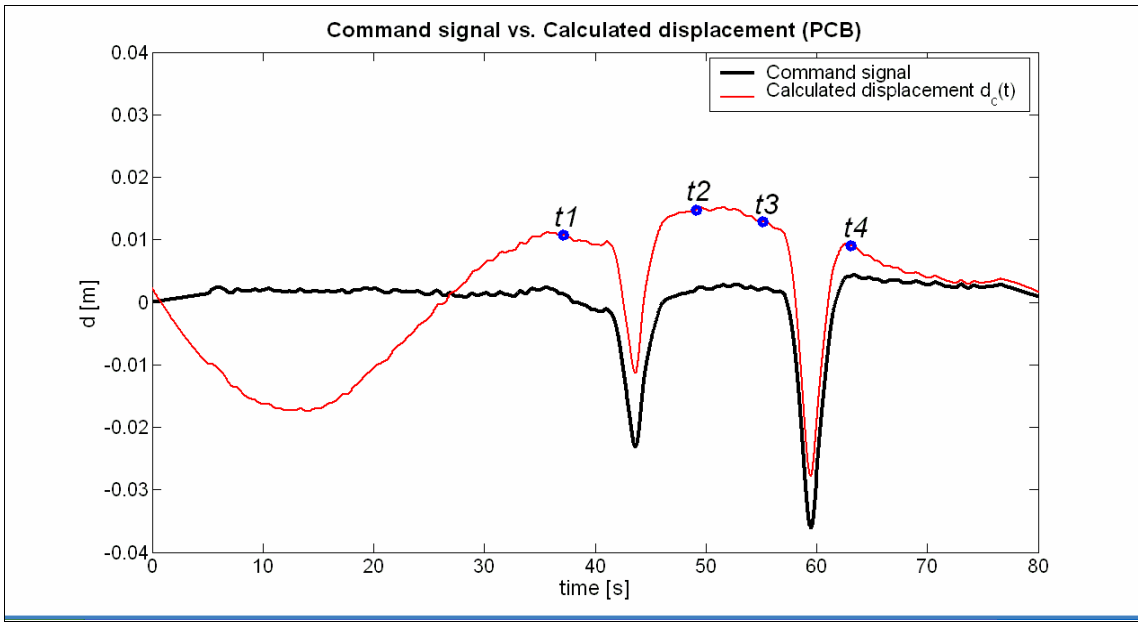

Figure 8 Results for test N4, PCB sensor. Calculated displacement including a linear interpolation at the events $d_{c\_rec}(t)$ vs. command signal.

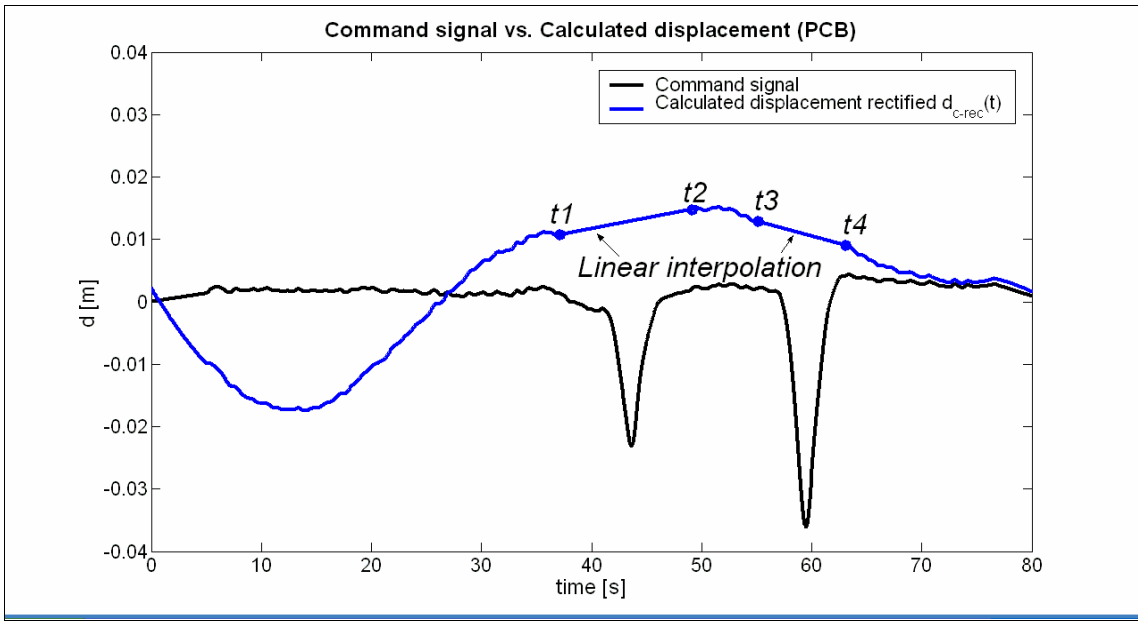

Figure 9 Results for test N4, PCB sensor. Polynomial approximation $p_n(t)$ used to approximate the base line drift vs. command signal.

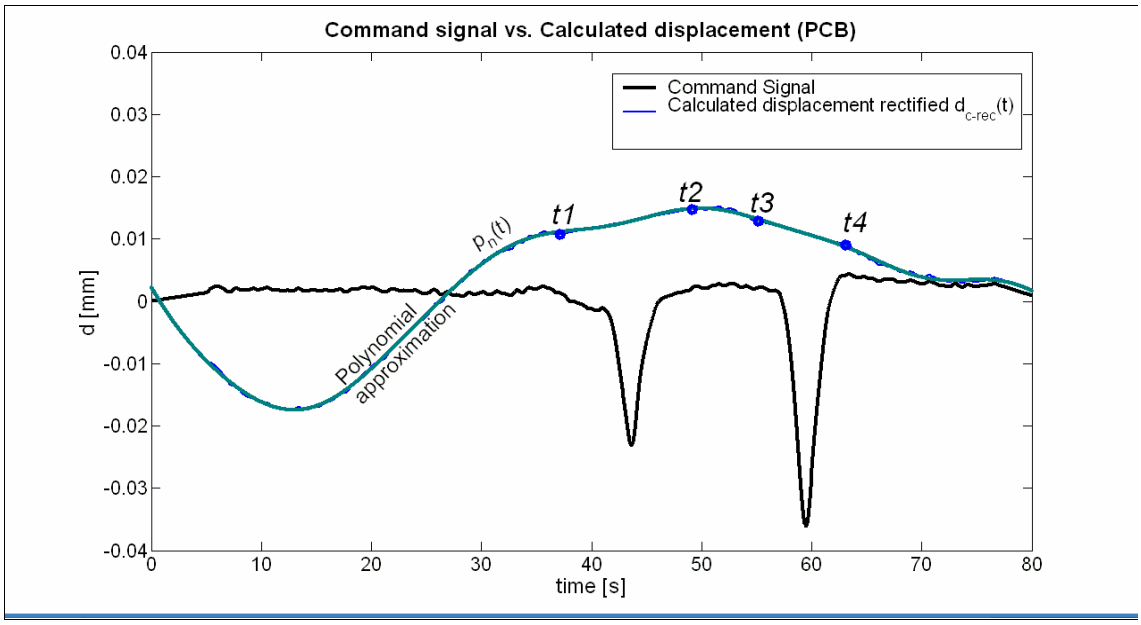

Figure 10 t. Results for test N4, PCB sensor. Calculated displacement after correction $d_{cc}(t)$ vs. command signal

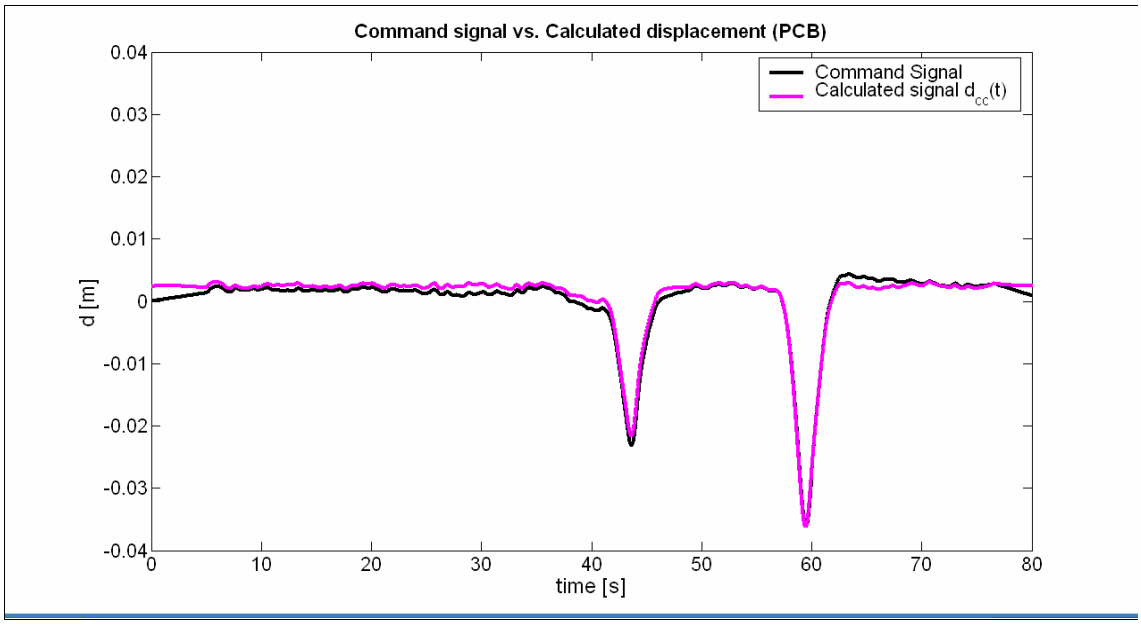

For all the tests, it was possible to reconstruct the displacement signal with quite good accuracy. Both selected sampling frequencies seem to have no influence on the results. For this purpose, PCB sensors showed a better performance and were therefore chosen for further testing at real scale. However, results of this baseline correction technique should be used carefully. The final results are sensitive to the fact that it is difficult to define the boundaries, i.e. when the event starts and ends. In addition small changes on these boundaries may produce significantly different results on the deformation traces. It is also necessary to find a way to define and evaluate the events automatically, as in a real application with thousand of registered measurements manual data evaluation would be impossible. The grade of the polynomial function used to approximate the baseline drift of the calculated signal affects the final results as well. In this case a polynomial function of grade 20 was chosen in order to better approximate the error of the calculated displacements. To overcome the problem of manual data evaluation a procedure had to be established, as shown later in section 5.3.

5. Full scale tests

5.1 Setup

Next step was to test PCB sensors and the correction algorithm for a real application. The sensors were installed within the different pavement structures of a specially prepared pavement on the ETH - IGT Circular Pavement Test Track (CPTT)[3] at Empa.

The CPTT is used as a full scale simulator for different pavement types. It uses three arms with loaded tires to simulate heavy traffic loads. The geometry of the device is schematically depicted in Figure 11. PCB accelerometers were installed in five different pavement structures A1 to A5 and measurements were performed for two different tire speeds: 20km/h and 50km/h. The sensors were mounted in a 50mm hole at 40mm depth of a 290mm thick asphalt pavement (see Figure 12). In this paper, only the data of A1 are discussed.

Figure 11 Schema of the CPTT, showing the 3 arms with their tires and the places A1 to A5 where the accelerometers were mounted for the tests.

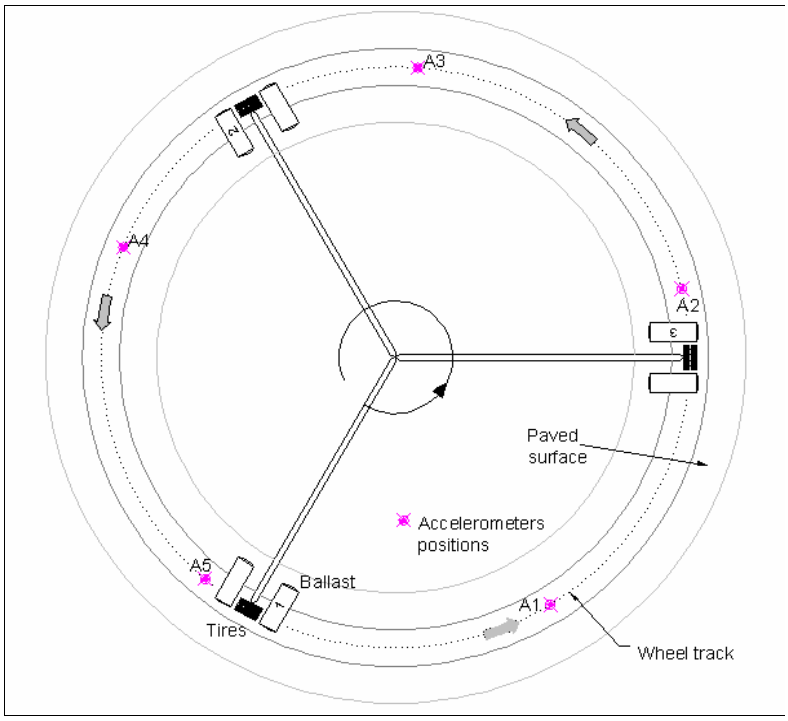

[3] The machine belongs to the Institute for Geotechnical Engineering (IGT) of the Swiss Federal Institute of Technology Zurich (ETH)

Figure 12 Detail of one of the sensors (left) and a broad view of the setup (right).

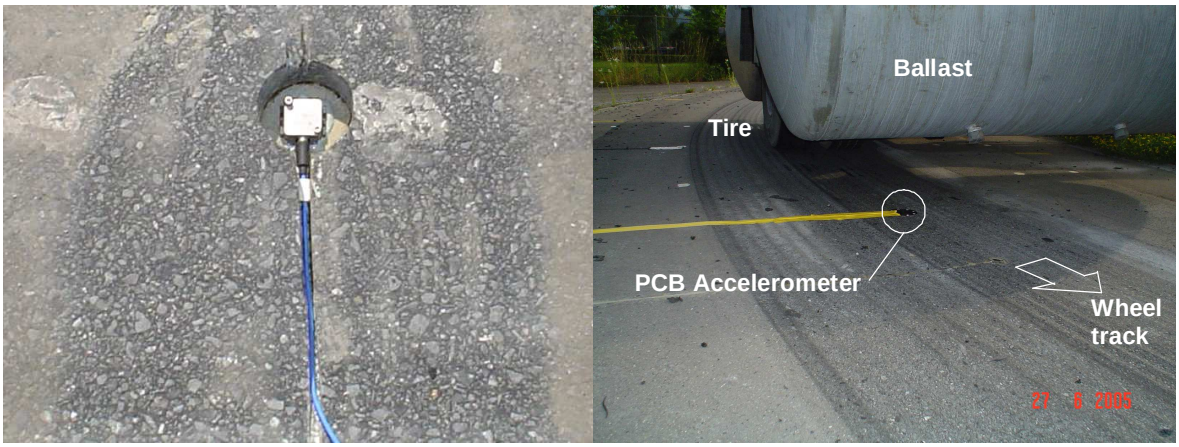

5.2 Experimental program

For each arm of the device (1,2,3), each position of the sensor (A1, A2, A3, A4, A5) and each velocity (20km/h and 50km/h) the measurements were repeated three times. Unfortunately, due to technical problems during the test, not all the data are available since tests of sites A3 and A4 had to be discarded.

Measurements were automatically triggered when acceleration values reached a threshold, and a measuring time window of 5s was recorded each time comprising 2,5s of pre-trigger measurements. The sampling rate used for these test was 2000Hz. Each acceleration record was therefore composed of 10000 samples.

5.3 Results

The direct integration of the acceleration traces revealed a drift of the calculated deflection as expected. In order to remove the deflection drifts, the same procedure as in the laboratory test was used but with two improvements: instead of using a linear interpolation during the event, a quadratic function (spline) was considered. By doing this, the polynomial curve was “softer” and probably followed more accurately a random drift (see Figure 13). Another improvement was the implementation of an empirically developed algorithm for automatic detection of the initial and end points of the event t_1, t_2. This algorithm is based on the calculation of the sliding root mean square (rms) of the acceleration signal for all recorded values using the following formula:

$$a(\tfrac{n+i}{2})_{rms} = \sqrt{\frac{\sum_{i=1}^{n} a(i)^2}{n}} \quad (7)$$

where:

$a(\frac{n+i}{2})_{rms}$: calculated sliding root mean square (rms) of the acceleration signal corresponding to the (n+i)/2 sample of the acceleration waveform

a (i) : ith sample of the acceleration waveform

n : the uneven number of samples used for the calculation of the rms

The rms is used to describe the "smoothed" vibration amplitude, as it is an average of the square amplitude of the signal. The sliding rms was calculated over a moving time window of 0,5s comprising the uneven number of n samples. The resulting value a_{rms} was assigned to the value corresponding to the middle of the window (n+i)/2. In this case, together with a defined threshold, the rms produced good results for the event duration.

Using this procedure, and setting a threshold of 0.015m/s2 for the test at 50km/h and a threshold of 0.006m/s2 for 20 km/h, the deflections of all measurements were calculated. Figure 14 and Figure 15 show the results for pavement A1 and tires 1 and 2 for 50km/h and 20km/h respectively. The first window shows the acceleration traces with their superimposed rms. The middle window contains the calculated deflection with the peak value. The shapes of the calculated deflection time histories are asymmetric in a similar way to those that can be found in the literature for viscoelastic materials. Amplitude and size of the deformation time history present a clear relation to the speed of the tire. The lower window shows the Power Spectrum (PS) of the signal. The dominant frequencies for the 50km/h tests are between 1Hz and 30Hz, with a peak around 11Hz. For the 20km/h tests, dominant frequencies are between 1Hz and 20Hz with a peak near 6Hz. For tire 1 there are higher frequencies peaks as well. For 50km/h these peaks are between 65Hz and 85Hz and for 20km/h are between 30Hz and 40Hz. This means that tire 1 is inducing some high frequency noise, probably due to an unbalanced rolling of the arm. As discussed in the introduction, these high frequency accelerations are strongly reduced by time integration and don't influence on the resulting deflection.

Figure 13 Calculated deflection and rms of the acceleration signal (dotted line). When the rms exceeds the threshold, it is said that the event starts at t_1 or ends at t_2. A spline is used for interpolation between these points.

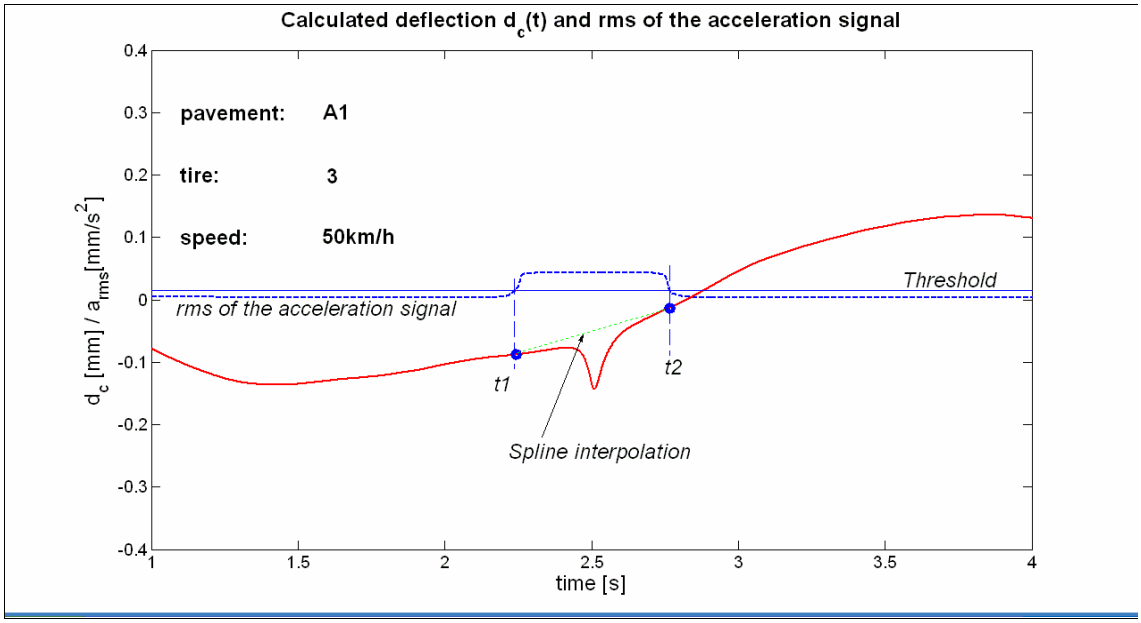

Figure 14 Acceleration traces and rms of the acceleration signal, calculated deflection and PS analysis corresponding to tests in pavement A1, for 50km/h and for tires 1 (top) and 2 (bottom). The PS shows the high frequency rolling vibration between 65Hz and 85Hz induced by tire 1. The integration of these high frequencies doesn't contribute to the calculated deflections.

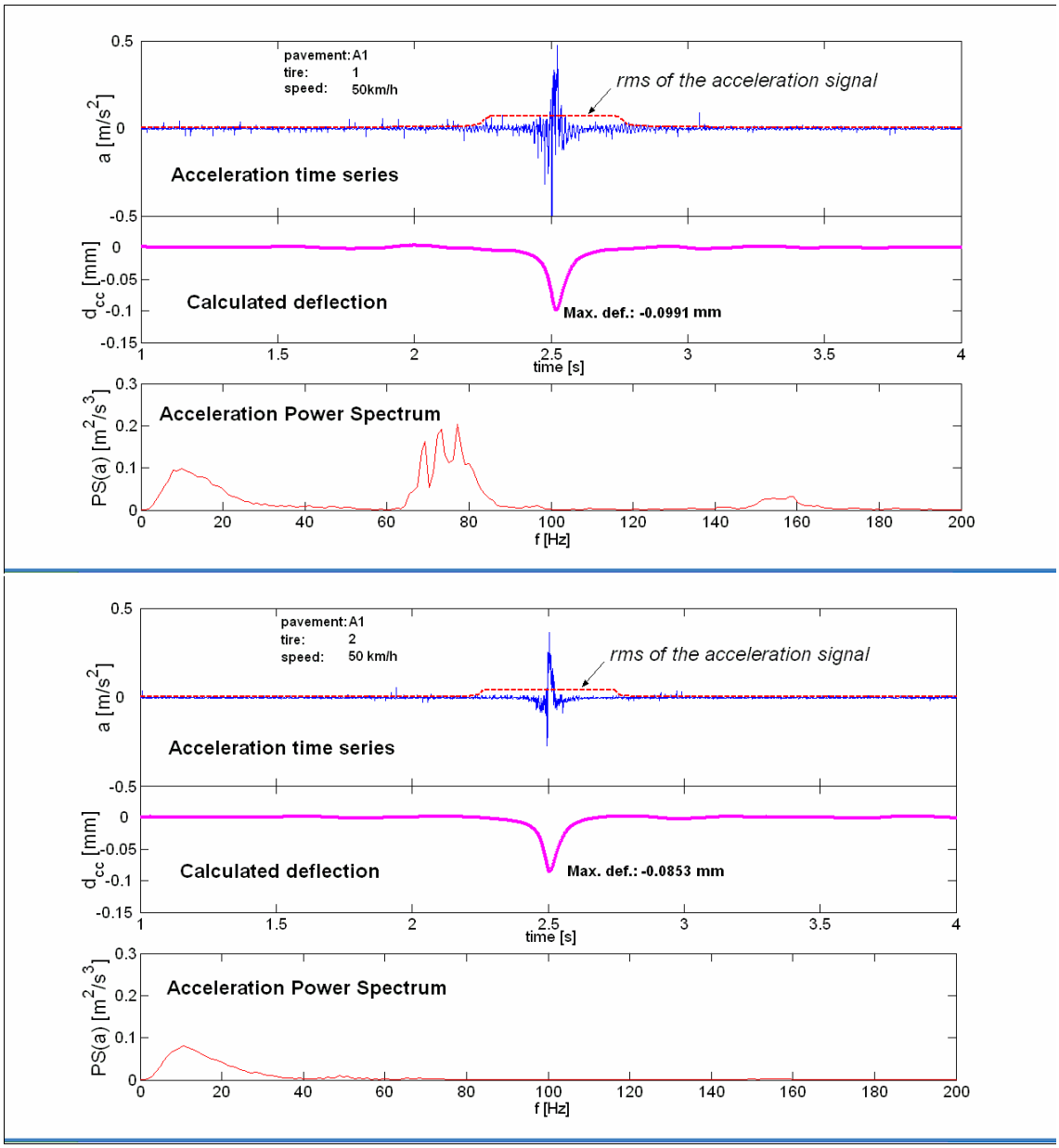

Figure 15 Acceleration traces and rms of the acceleration signal, calculated deformation and PS analysis corresponding to tests in pavement A1, for 20km/h and for tires 1 (top) and 2 (bottom). For this speed, vibrations of tire 1 induce frequencies between 30Hz and 40Hz.

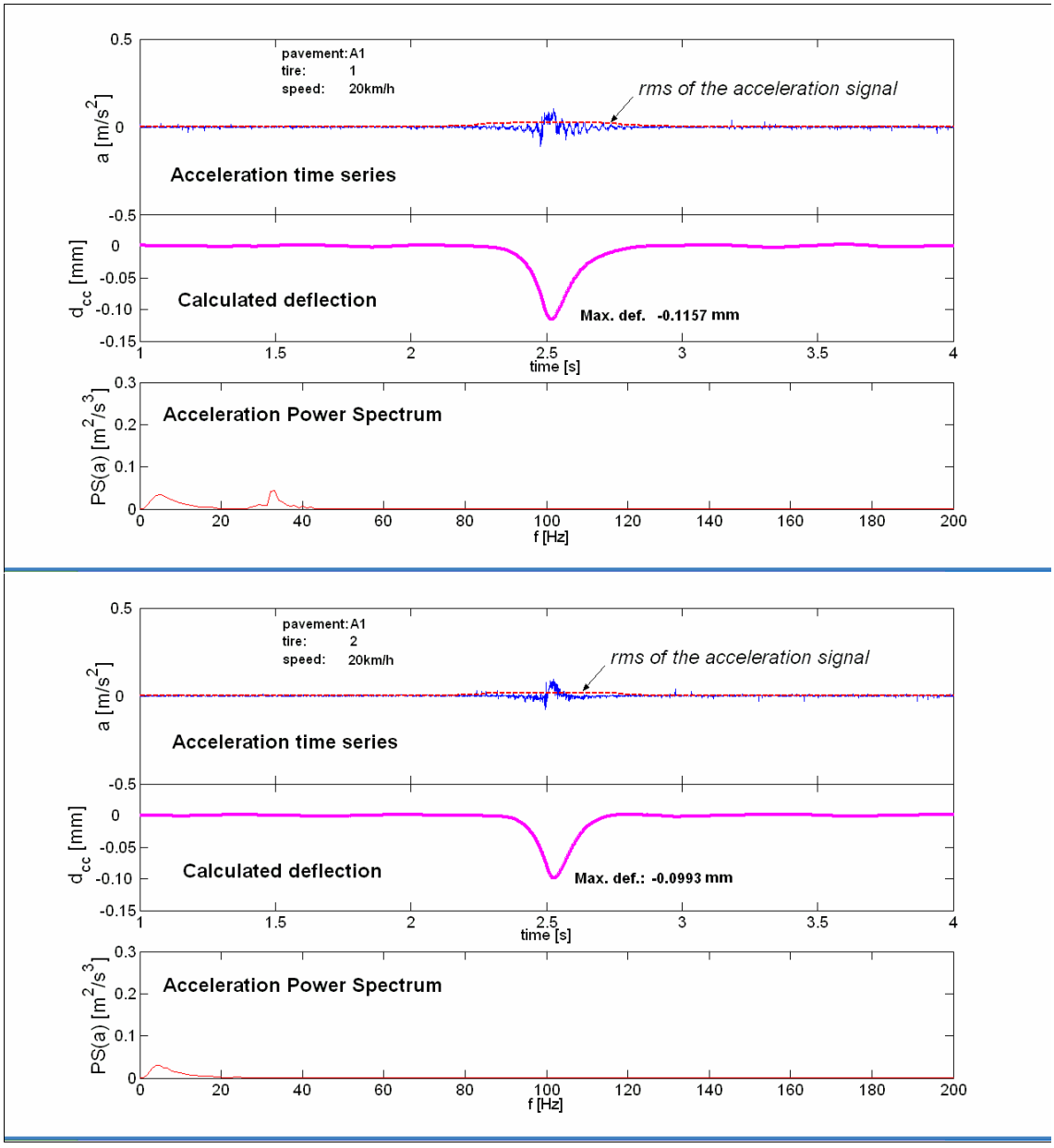

Table 3 shows the peaks for measurement in site A1, the average value of the three tests performed (mean A) and a final average for each pavement site and speed, without considering the tire number (mean B).

Table 3 Calculated deflection peaks and average for each speed and tire for measuring site A1..

Point	Speed [km/hr]	Tire	meas 1 [mm]	meas 2 [mm]	meas 3 [mm]	mean A	mean B
A1	20	1	0.116	0.116	0.110	0.114	0.109
		2	0.111	0.099	0.104	0.105	
		3	0.108	0.114	0.105	0.109	
	50	1	0.087	0.083	0.099	0.090	0.085
		2	0.085	0.086	0.078	0.083	
		3	0.077	0.085	0.082	0.081	

Measured peaks confirm the viscous nature of the asphalt materials of the pavement, as lower tire speeds produce larger deflection peaks. Although the results regarding peak values seems reasonable, they should be considered carefully as no validation measurement or model was done up to now.

6. Conclusions and following steps

In order to develop simple, reliable methods for measuring in situ vertical deformation of pavements under real traffic, the use of accelerometers was evaluated. It was shown that the conversion of acceleration into deflections using numerical double integration can be done successfully. Possible problems of time integration were identified and the origin of these problems described. In particular it was demonstrated that the amplification of low frequency errors of the recorded acceleration leads to unacceptable deflection baseline drifts.

In order to attenuate the errors, the use of accelerometers capable to measure low frequency signals with high resolution was proposed and tested in the laboratory. With the intention of correcting the inevitable resulting errors, a polynomial function was selected to approximate the calculated deflections before and after the events. No filtering was used. The polynomial function was then subtracted to the whole signal providing quite reasonable results.

Hence, a full scale test was carried out and accelerometers were installed in the ETH – IGT Circular Pavement Test Track. A method for automatically detecting the passing tire using the root mean square of the acceleration signal was implemented in a satisfactory way. However, up to now only the method to determine road deflections from traffic induced accelerations could be presented. A validation using finite elements will be implemented in the next step of this ongoing research study. Furthermore, tests in a motorway are planned and deformation sensors will be used to validate the measurements in the field.

7. Acknowledgments

The authors would like to thank Peter Anderegg, Glauco Feltrin, Felix Weber and Daniel Gsell from Empa, for their discussions, suggestions and valuable help during the laboratory tests. We would like to thank the Institute for Geotechnical Engineering (IGT) of the Swiss Federal Institute of Technology Zurich (ETH), specially Carlo Rabaiotti and Markus Caprez, for allowing us to use the CPTT. Our gratitude is also to our department colleagues Hans Kienast and Christian Meierhofer, for preparing the measurement set up at the CPTT.

8. References

Boore, D. M. (2001), "Effect of baseline corrections on displacements and response spectra for several recordings of the 1999 Chi-Chi, Taiwan, earthquake", *Bull. Seism. Soc. Am*., 91, 1199—1211,

Boore, D. M.(2002), Stephens, C. D., and Joyner, W. B., "Comments on baseline correction of digital strong-motion data: Examples from the 1999 Hector Mine, California, earthquake", *Bull. Seism. Soc. Am*., 92, 1543—1560

Boore, D. M.(2003), "Analog-to-digital conversion as a source of drifts in displacements derived from digital recordings of ground acceleration", *Bull. Seism. Soc. Am*., 93, 2017—2024

Boore D. M., "Long-period ground motions from digital acceleration recordings: a new era in engineering seismology", *Proc. International Workshop on Future Directions in Instrumentation for Strong Motion and Engineering Seismology*, Kusadasi, Turkey, Kluher, Dordrecht, The Netherlands (in press), May 17–21, 2004

Chiu H.-C. (1997), "Stable Correction of Digital Strong-Motion Data", Bulletin of the Seismological Society of America, Vol. 87, No. 4, pp. 932-944, August

Feltrin G., Gsell D. and Weber F (2004)., "Berechnung von Verschiebungen mittels Zeit-Integration gemesser Beschleunigungen :Eine kleine Untersuchung", *7. Symposium Bauwerksdynamik und Erschütterungsmessungen*, Empa Akademie Dübendorf, 4.6.2004

Iwan, W.D., Moser M. A., Pen C.-Y. (1985), "Some observations on strong-motion earthquake measuring using a digital accelerograph" *Bulletin of the Seismological Society of America*, 75, 1225-1246,

Raab, C., Partl, M. N., Anderegg, P., Brönnimann, R (2003)., "Two Years Experience with a New Long-Term Pavement Performance Monitoring Station on a Swiss Motorway", *Proceedings of 3rd International Symposium on Maintenance and Rehabilitation of Pavements and Technological Control*, 7th-10th July 2003, Minho University, Guimarães, Portugal, pp263-271

Raab, C, Poulikakos, L., Anderegg, P, Partl, M.N (2002), "Long-Term Pavement Performance Monitoring of a Swiss Motorway", *Proceedings of the Third International Conference on Weigh-in-Motion (ICWIM3)*, 13th - 15th May 2002, Orlando, Florida, ISBN 0-9652310-5-4, pp335-340

Shieh J., Huber J.E., Fleck N.A., Ashby M.F. (2001) , "The selection of sensors", *Progress in Material Science*, 46, 461-504